PHYSICAL REVIEW B VOLUME 58, NUMBER 12 15 SEPTEMBER 1998-II

Spatial evolution of hot-electron relaxation in quantum Hall conductors

I. I. Kaya, G. Nachtwei, K. von Klitzing, and K. Eberl
Max-Planck-Institut für Festkörperforschung, Heisenbergstraße 1, D-70569 Stuttgart, Germany
(Received 27 January 1998)

We have analyzed the energy relaxation of hot electrons in the prebreakdown regime of the quantum Hall effect. Hot electrons, generated by a periodic set of constrictions, are injected into two-dimensional electron systems (2DES's) of various mobilities, with Hall fields below the breakdown value. The resistivity of the 2DES is measured as a function of the distance from the injection front. The results are compared with calculations on the basis of a nonequilibrium between the excitation and relaxation of hot electrons. Energy relaxation lengths from 0.3 to 3 μm were deduced, which increase with the mobility and are comparable to the mean free path. [S0163-1829(98)51936-4]

The nondissipative current flow in the quantum Hall[1] (QH) regime is restricted to a certain current range, limited by a critical current.[2] Above this critical current value, which depends on geometrical[3–5] and intrinsic[5,6] sample properties, a sudden onset of dissipation with an abrupt increase of the resistivity ρ_{xx} [breakdown of the quantum Hall effect (QHE)] occurs.

In samples with mobilities in the range 10^5-10^6 cm^2/V s, a linear dependence of the critical current on the sample width was found.[5] This result implies a constant critical current density and indicates the relevance of intrinsic two-dimensional (2D) bulk properties for the breakdown. Besides this rather predictable *width* dependence, a peculiar *length* dependence of the QHE breakdown was recently reported.[7] Moreover, it was found that the breakdown develops over a certain drifting distance of electrons in the device, visible as an increase of resistivity (and hence energy dissipation) along the drift direction of electrons.[8] This result is explained on the basis of an avalanche heating process of the electrons, reaching a steady state of balanced energy gain and loss after a certain drifting distance.

In this study, we have monitored the decay of the energy of hot electrons along their drift path by measurements of the resistivity as a function of the distance from the position of hot-electron injection. The electrons are heated in arrays of parallel narrow channels (wires). These wires form a series of parallel constrictions with equivalent properties, providing a homogeneous temperature front of heated electrons that enter the unpatterned two-dimensional electron system (2DES). A set of logarithmically spaced, narrow potential probes was used to monitor the resistivity profile, which is related to the energy relaxation of the hot electrons inside the 2DES. We found remarkable dependences of the resistivity profile on the current and on the electron mobility of the samples. Within a small range of currents below the critical value, a strong increase of the characteristic decay length of the resistivity was observed. Above a certain current level, the dissipation persists over the entire sample length. For electrons injected from a wide metallic contact (opposite current direction), the QH breakdown was found at higher currents.

The samples were prepared from four GaAs/$Ga_xAl_{1-x}As$ wafers with electron densities n_s ranging from $n_s=2.0$ to 2.6×10^{11} cm^{-2} and Hall mobilities μ_H in the range from $\mu_H=4.0\times10^4$ to 1.04×10^6 cm^2/V s. The samples were selected to cover a wide range of mobilities at nearly the same carrier density. The various mobilities were realized by different spacer thicknesses. All samples were patterned as Hall bars of a width of $w=90$ μm with 19 pairs of Hall probes (2-μm wide at the junction to the current channel), logarithmically spaced from $l=6$ μm to 133 μm. For the heating of electrons, 100-μm-long grooves of 2-μm effective width, leaving 2-μm-wide channels (wires) in between, were patterned by electron beam lithography periodically and in parallel to the current flow direction (see Fig. 1). In comparison to a single constriction of the same width ratio, the periodic arrangement of wires produces more uniform electron temperatures at the end of the constricted area.

At all samples, current- and temperature-dependent measurements of the quantum transport were performed in the current range from $10\ \mu A\leqslant|I_{SD}|\leqslant55\ \mu A$ (for both current polarities), at temperatures $1.3\ K\leqslant T\leqslant18$ K and and in magnetic fields $|B|\leqslant11.5$ T (for both field directions).

Figure 2 shows the resistivity $\rho_{xx}=(V_x/I_{SD})(w/l)$ as a function of the magnetic field near the second QH plateau, for a current I_{SD} well below the critical current $I_c^0=45$ μA. The parameter x indicates the position of the resistivity measurement (in the middle between two adjacent potential probes) relative to the injection front at the end of the wires (see Fig. 1). No significant changes of the resistivity ρ_{xx} as a function of the probing position x were observed for the current flow direction towards the wires [in our notation, the current flow direction is identical with the direction of electron motion, Fig. 2(a)]. In contrast, the electron injection through the wire array into the Hall device leads to a strong

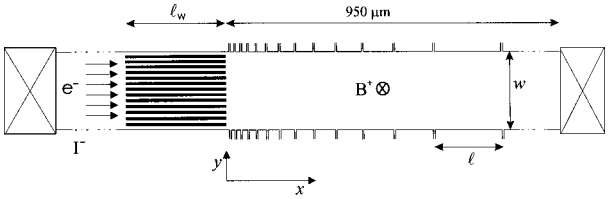

FIG. 1. Schematic view of the sample geometry. l_w is the length of the wires, w is the width of the quantum Hall conductor, and l is the distance between the potential probes.

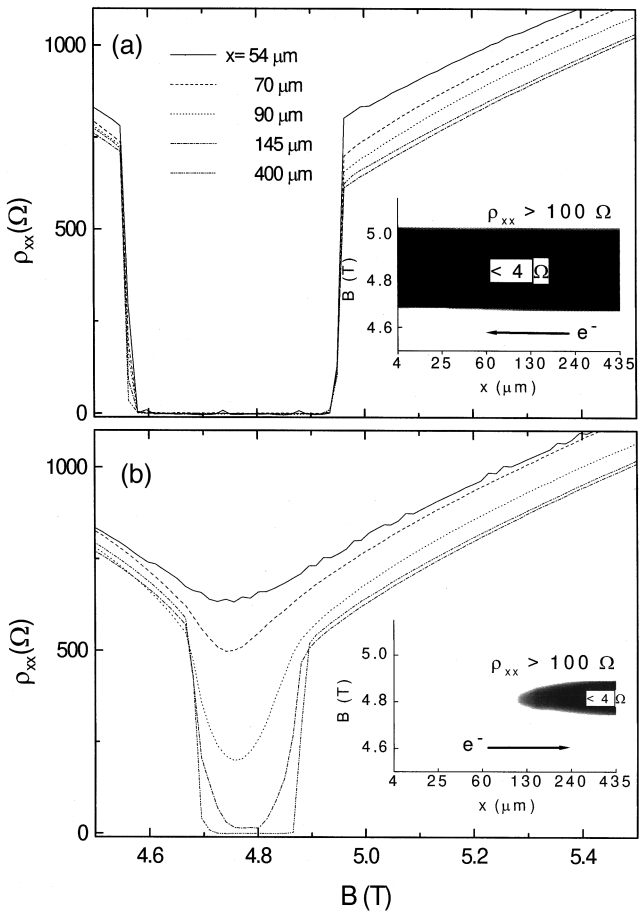

FIG. 2. Resistivity ρ_{xx} of sample *A* near the second QH plateau, measured at different pairs of adjacent potential probes with current flow of electrons *towards* [(a) $I=+35\,\mu$A] and *from* [(b) $I=-35\,\mu$A] the wire array. The distance of the potential probes from the wire array is given in the legend. Insets: gray-scale plots of ρ_{xx} (black: $\rho_{xx}\leqslant 4\,\Omega$, white: $\rho_{xx}\geqslant 100\,\Omega$) in dependence on the magnetic field B and probing position x (taken in the middle between the adjacent potential probes). Only for the current flow from the wires into the 2DES, does a significant distance dependence of ρ_{xx} occur.

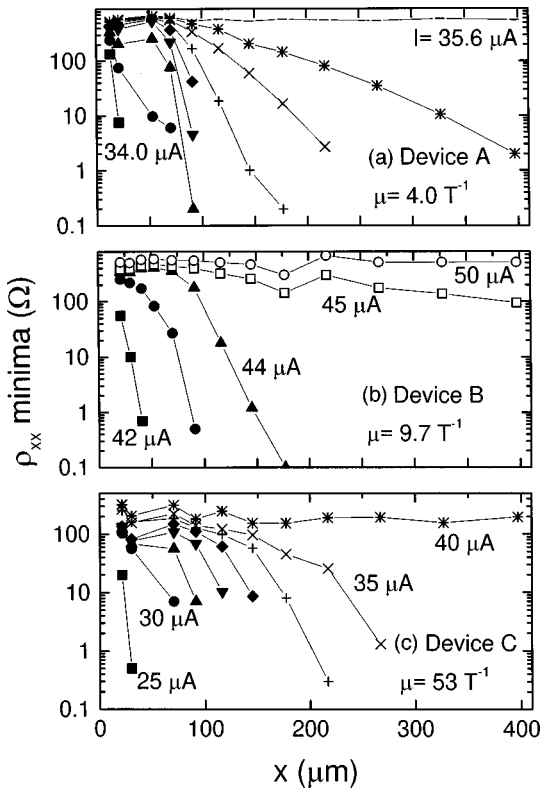

FIG. 3. Dependence of the ρ_{xx} minimum on the distance of the probing contacts from the end of the wire array at different currents. (a) Sample *A*, $I=34.0\,\mu$A (square), 34.2, 34.4, 34.6, 34.8, 35.0, 35.2, 35.4, and 35.6 μA (dashed line). (b) Sample *B*, $I=42\,\mu$A (squares), 43, 44, 45, and 50 μA (open circles). (c) Sample *C*, $I=25\,\mu$A (squares), 30, 31, 32, 33, 34, 35, and 40 μA (stars).

dependence of ρ_{xx} on the probing position x, as shown in Fig. 2(b). The farther the potential probes are located away from the hot-electron entrance at the end of the wires, the wider the QH plateau becomes [see the inset in Fig. 2(b) with a gray-scale plot of ρ_{xx} in the B-x plane]. These plots clearly demonstrate that hot electrons, heated in the wire array ($\rho_{xx}>100\,\Omega$), penetrate deeply into the device over length scales up to hundreds of micrometers. This is a clear indication that a certain drifting distance is necessary for the hot electrons to relax to the lattice temperature. The same principal behavior was observed for all samples, but on a length scale increasing with the sample mobility. In Fig. 3, the variation of ρ_{xx} at the filling factor $\nu=2$ as a function of the probing position x is shown for samples *A*, *B*, and *C* [Figs. 3(a)–3(c), for the sample parameters see Table I], with the current as parameter. At lower currents, ρ_{xx} decreases rapidly with the distance towards $\rho_{xx}=0$ (within the uncertainty of the measurement). With increasing current, the slope of ρ_{xx} as a function of the distance decreases. The function $\rho_{xx}(x)$ can be approximated by an exponential dependence:

$$\rho_{xx}(x)=\rho_{xx}^{0}\exp\left\{-\frac{x-x_0}{L_0}\right\} \tag{1}$$

in the region with $x>x_0$ where ρ_{xx} is smaller than a certain saturation value ρ_{xx}^{0}, which is of the order of some hundred ohms. The value of x_0 marks the end of the saturation area near the injection front. This saturation area ($0<x<x_0$) is mainly due to a weaker temperature dependence of ρ_{xx} at rather high electron temperatures, present close to the injection front. L_0 is the characteristic decay length of the resistivity. The resistivity profiles $\rho_{xx}(x)$ could be better approximated by Eq. (1) for the samples with lower mobilities. For sample *D* with the highest mobility, the gray-scale plot of $\rho_{xx}=f(B,x)$ (Fig. 4) clearly shows a strong inhomogeneity of the QH state along the sample around the filling factor $\nu=2$. In this case, no clear functional dependence $\rho_{xx}(x)$ could be deduced, although the principal behavior is similar to that of the samples with lower mobility.

From Fig. 3, a clear trend of the ρ_{xx}-vs-x slope towards zero with increasing current is visible for samples *A*, *B* and *C*. The corresponding characteristic decay length L_0 is a function of the current *I*, tending to infinity at a certain current. This current is identical with the breakdown current I_c^{-}, injected from the wire array into the unpatterned region. In this case, the hot-electron state persists over the entire sample, representing a stationary equilibrium of the energy gain rate of electrons from the electric field E_x along the current flow direction and the corresponding loss due to

TABLE I. All data in the table are given for one magnetic field direction. For the opposite direction (values in brackets for l_D), the values agree within experimental error. The critical currents were measured approximately in the middle between the wire array and the metallic current contact.

Sample	$n_s/10^{15}$ m^{-2}	μ_H/T^{-1}	l_{mfp}/μm	I_c^+/μA	I_c^-/μA	τ_0/ns	l_D/μm
A	2.25	4.0	0.31	45	35.4	0.24	0.26 (0.27)
B	2.6	9.7	0.82	53	45.2	0.46	0.55 (0.64)
C	2.0	53	3.9	37	36.6	2.60	3.2 (4.0)
D	2.15	104	7.9	48	48		

dissipation. For currents $I<I_c^-$ (all currents are meant as absolute values unless stated explicitly), $L_0(I)$ is finite, representing a nonequilibrium with the dissipative loss dominating over the energy gain:

$$R_{xx}I^2<\{E(T_e)-E(T_L)\}/\tau_0, \tag{2}$$

with $R_{xx}=\rho_{xx}l/w$, $E(T)$ as the energy of the electron system at the elevated electron temperature T_e or the lattice temperature T_L, respectively, and τ_0 as the energy relaxation time of the heated electrons. Due to this nonequilibrium, the hot electrons injected from the wire array continuously lose energy while drifting through the sample, until they equilibrate with the lattice temperature and return to the (nearly) nondissipative QH state. To relate this equilibrium process to the sample current and the scattering, we apply a two-level model for the relaxation process of hot electrons. A 2DES at an integer filling factor in thermodynamic equilibrium at $T=0$ is characterized by a Fermi energy E_F in the middle between two Landau levels. All electrons populate the levels below the Fermi energy, leaving the upper level at $E_F+\frac{1}{2}\hbar\omega_c$ (spin splitting neglected for even filling factors) empty. Thus, the longitudinal resistance R_{xx} of such a system is zero. If electrons are activated (thermally or by electric fields) to the upper level, the resistance R_{xx} is proportional to the number N of activated electrons: $R_{xx}=\gamma N$. Due to the energy loss processes (as, e.g., electron-phonon scattering), a population of N electrons in the upper level will decay in time on a typical time scale of τ_0. Consequently, the entire differential change of the population in the upper level can be written as

$$dN=dN_{\mathrm{gain}}-dN_{\mathrm{loss}}=\frac{R_{xx}I^2dt}{\hbar\omega_c}-N\frac{dt}{\tau_0}, \tag{3}$$

based on the assumption that the energy gain $R_{xx}I^2dt$ is used to elevate dN_{gain} electrons over the Landau gap $\hbar\omega_c$. To obtain the resistivity $\rho_{xx}(x)$ as a function of the drifting distance x, we substitute the drifting time t by x according to $dt=dx/\mathbf{v}_D$ ($\mathbf{v}_D$ is the drift velocity) and apply the relation $\rho_{xx}=\gamma N\cdot(w/l)$. Further, we define ρ_{xx}^0 as the resistivity in the saturation area ($0<x<x_0$) close to the end of the wire array and make use of our experimental observation that ρ_{xx} becomes independent of x for $I\geqslant I_c$. Applying these assumptions and Eq. (3), $\rho_{xx}(x)$ can be deduced:

$$\rho_{xx}(x)=\rho_{xx}^0\exp\left\{-\frac{x-x_0}{l_D}\left[1-\left(\frac{I}{I_c}\right)^2\right]\right\}, \tag{4}$$

with $l_D=\mathbf{v}_D\tau_0$ as the average drifting length of electrons between two inelastic scattering events (energy relaxation length) and $I_c^2=\hbar\omega_c/\gamma\tau_0$.

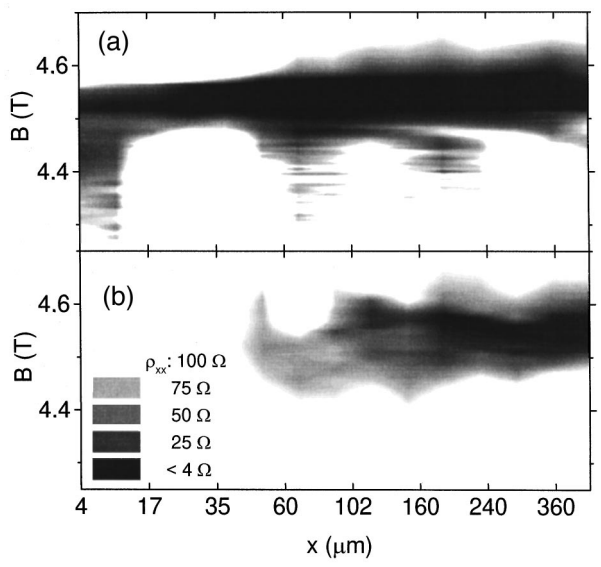

FIG. 4. Gray-scale plots of ρ_{xx} in dependence on the magnetic field B and probing position x for the high-mobility sample D [(a) $I=+35\ \mu$A and (b) $I=-35\ \mu$A]. Strong inhomogeneities along the current flow direction are evident from this plot. However, the qualitative behavior is similar to the samples with lower mobilities.

Comparing Eqs. (1) and (4), the characteristic decay length L_0 can be related to the sample current I and the energy relaxation length l_D according to $L_0=l_D/[1-(I/I_c)^2]$. From the plots of $\ln(\rho_{xx})$ vs x as shown in Fig. 3, we deduce L_0 from the linear part of the plot (typically in the range $1\ \Omega<\rho_{xx}<100\ \Omega$). The linearity of these plots was found the better, the lower the mobility and the closer to the breakdown the current was. To determine l_D from our measurements, we plot $1/L_0$ as a function of $(I/I_c)^2$ (Fig. 5). As visible from Fig. 5, these plots yield approximately linear dependences for the samples *A*, *B*, and *C* (lower mobilities) in a current range of $\Delta I/I_c\approx 5-25\,\%$ (the observable range increases with mobility). The corresponding values for l_D are summarized in Table I and show a remarkable coincidence with the mean free path l_{mfp}. As the latter values are mainly determined by *elastic* Coulomb scattering at ionized donors (at $B\rightarrow 0$ and $T=1.3$ K), this means that the *inelastic* scattering (responsible for the dissipation near the QHB breakdown) is also related to the scattering at ionized donors. This can be attributed to a high scattering probability of electrons, incident from the x direction, into the y direction (parallel to the Hall electric field) by Coulomb scattering, followed by an inelastic scattering event along the Hall field.

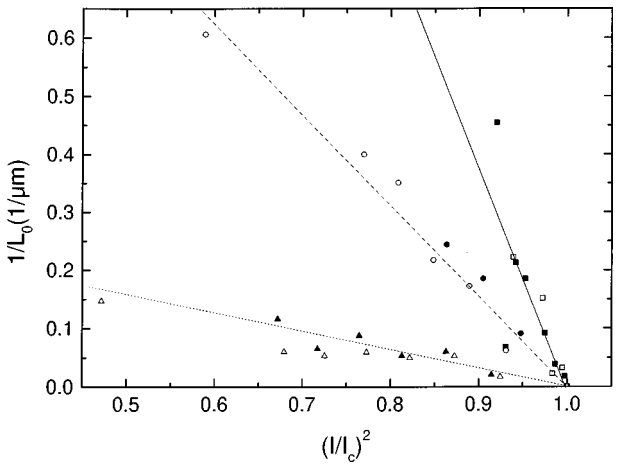

FIG. 5. Plots of the inverse characteristic decay length $1/L_0$ versus $(I/I_c)^2$ for samples *A* (squares), *B* (circles), and *C* (triangles) for both orientations of the magnetic field (full and open symbols). From these plots, the energy relaxation lengths and energy relaxation times can be determined.

From the values of the energy relaxation length l_D and the drift velocity $\mathbf{v}_D$, the energy relaxation time τ_0 can be determined. As the breakdown currents are comparable for the samples *A*, *B*, and *C*, the values of τ_0 at $I=I_c$ were found proportional to the mean free path or the Hall mobility of the samples, respectively (see Table I). The order of magnitude of the energy relaxation times (0.24–2.6 ns) is in good agreement with earlier assumptions,[9] which were explained by phonon-assisted dissipation. However, the observed proportionality between energy relaxation time and Hall mobility means that the inelastic scattering rate in our samples is dominated by the scattering at impurities instead of intrinsic electron-phonon coupling properties of the GaAs-bulk. Fal'ko and Challis have calculated inter-Landau-level relaxation rates for a 2DES in GaAs for one-phonon and two-phonon emission processes.[10] They considered deformation and piezoelectric electron-phonon coupling. At higher magnetic fields, as relevant for our experiments, they predict a dominance of two-phonon emission (with opposite directions of the wave vectors of the emitted phonons) for the inter-Landau-level relaxation. This was explained by the requirement of momentum conservation, which leads to a suppression of one-phonon processes with decreasing magnetic length. Applying the corresponding relations, derived by Fal'ko and Challis, we obtain inter-Landau-level relaxation times of 80 ns for the two-phonon process and 9 μs for the one-phonon process for magnetic fields corresponding to the second QHE plateau. These values exceed the energy relaxation times, which were observed in our experiments, by orders of magnitude and can therefore be taken as a confirmation of the importance of impurity-induced scattering for the energy relaxation near the breakdown of the QHE.

To summarize, we have measured the spatial evolution of the hot-electron relaxation in a 2DES in quantizing magnetic fields. The electrons were heated in a wire array to provide a uniform electron temperature at the injection front. The characteristic decay length of the resistivity was found to strongly increase with current in a rather narrow range of currents. For currents above the critical value, the resistivity remains elevated and almost unchanged over the entire sample length ($\approx$1 mm). The characteristic decay lengths (at comparable currents slightly below the breakdown value) were found the longer, the higher the sample mobility is. The current dependence of the characteristic decay length was explained by the energy loss dominating over the energy gain of electrons. A clear correlation of the energy relaxation lengths and the energy relaxation times with the mean free path was found, indicating the relevance of Coulomb scattering at ionized donors for the breakdown of the QHE.

The authors would like to acknowledge valuable discussions with W. Dietsche and R. R. Gerhardts.

[1] K. von Klitzing, G. Dorda, and M. Pepper, Phys. Rev. Lett. **45**, 449 (1980).

[2] G. Ebert, K. von Klitzing, K. Ploog, and G. Weimann, J. Phys. C **16**, 5441 (1983).

[3] M. E. Cage, R. F. Dziuba, B. F. Field, E. R. Williams, S. M. Girvin, A. C. Gossard, D. C. Tsui, and R. J. Wagner, Phys. Rev. Lett. **51**, 1374 (1983).

[4] L. Bliek, E. Braun, G. Hein, V. Kose, J. Niemeyer, G. Weimann, and W. Schlapp, Semicond. Sci. Technol. **1**, 110 (1986).

[5] S. Kawaji, H. Hirakawa, M. Nagata, T. Okamoto, T. Fukase, and T. Gotoh, Surf. Sci. **305**, 161 (1994).

[6] N. Q. Balaban, U. Meirav, H. Shtrikman, and Y. Levinson, Phys. Rev. Lett. **71**, 1443 (1993).

[7] Y. Kawaguchi, S. Komiyama, T. Osada, and Y. Shiraki, Physica B **227**, 183 (1996).

[8] S. Komiyama, Y. Kawaguchi, T. Osada, and Y. Shiraki, Phys. Rev. Lett. **77**, 558 (1996).

[9] S. Komiyama, T. Takamasu, S. Hiyamizu, and S. Sasa, Solid State Commun. **54**, 479 (1985).

[10] V. I. Fal'ko and L. J. Challis, J. Phys.: Condens. Matter **5**, 3945 (1993).